

MBD2 Mediates Septic AKI through Activation of PKC η /p38MAPK and the ERK1/2 Axis

Yuxin Xie,^{1,2,8} Bohao Liu,^{1,2,8} Jian Pan,^{1,2} Jiamiao Liu,² Xiaozhou Li,^{1,2} Huiling Li,³ Shuangfa Qiu,^{1,2} Xudong Xiang,^{1,2} Peiling Zheng,⁶ Junxiang Chen,⁴ Yunchang Yuan,⁵ Zheng Dong,^{4,7} and Dongshan Zhang^{1,2,4}

¹Department of Emergency Medicine, Second Xiangya Hospital, Central South University, Changsha, Hunan, People's Republic of China; ²Emergency Medicine and Difficult Diseases Institute, Second Xiangya Hospital, Central South University, Changsha, Hunan, People's Republic of China; ³Department of Ophthalmology, Second Xiangya Hospital, Central South University, Changsha, Hunan, People's Republic of China; ⁴Department of Nephrology, Second Xiangya Hospital, Central South University, Changsha, Hunan, People's Republic of China; ⁵Department of Chest Surgery, Second Xiangya Hospital, Central South University, Changsha, Hunan, People's Republic of China; ⁶Department of Endocrinology, Shenzhen People's Hospital, Second Clinical Medical College of Jinan University, First Affiliated Hospital of Southern University of Science and Technology, Shenzhen, People's Republic of China; ⁷Department of Cellular Biology and Anatomy, Medical College of Georgia at Georgia Regents University and Charlie Norwood VA Medical Center, Augusta, GA, USA

Our previous study demonstrated that the methyl-CpG-binding domain protein 2 (MBD2) mediates vancomycin (VAN)-induced acute kidney injury (AKI). However, the role and regulation of MBD2 in septic AKI are unknown. Herein, MBD2 was induced by lipopolysaccharide (LPS) in Boston University mouse proximal tubules (BUMPTs) and mice. For both *in vitro* and *in vivo* experiments, we showed that inhibition of MBD2 by MBD2 small interfering RNA (siRNA) and MBD2-knockout (KO) substantially improved the survival rate and attenuated both LPS and cecal ligation and puncture (CLP)-induced AKI, renal cell apoptosis, and inflammatory factor production. Global genetic expression analyses and *in vitro* experiments suggest that the expression of protein kinase C η (PKC η), caused by LPS, is markedly suppressed in MBD2-KO mice and MBD2 siRNA, respectively. Mechanistically, chromatin immunoprecipitation (ChIP) analysis indicates that MBD2 directly binds to promoter region CpG islands of PKC η via suppression of promoter methylation. Furthermore, PKC η siRNA improves the survival rate and attenuates LPS-induced BUMPT cell apoptosis and inflammatory factor production via inactivation of p38 mitogen-activated protein kinase (MAPK) and extracellular signal-regulated kinase (ERK)1/2, which were further verified by PKC η siRNA treatment in CLP-induced AKI. Finally, MBD2-KO mice exhibited CLP-induced renal cell apoptosis and inflammatory factor production by inactivation of PKC η /p38MAPK and ERK1/2 signaling. Taken together, the data indicate that MBD2 mediates septic-induced AKI through the activation of PKC η /p38MAPK and the ERK1/2 axis. MBD2 represents a potential target for treatment of septic AKI.

INTRODUCTION

Acute kidney injury (AKI) is a common complication of patients with sepsis.¹ It occurs in approximately 40%–50% of all septic patients and is associated with high mortality.^{2,3} Although extensive research has focused on sepsis-induced AKI,^{4–7} the underlying mechanisms

remain largely unknown, resulting in reactive and nonspecific therapy.

Numerous studies have reported that DNA methylation is associated with AKI induced by ischemic and nephrotoxic drugs.^{8,9} However, little is known about the role of DNA methylation in AKI. Guo et al.⁹ reported that DNA methyltransferase 1 (DNMT1) plays a renal-protective role in cisplatin-induced AKI. By contrast, our recent study suggests that methyl-CpG-binding domain protein 2 (MBD2), a key methylated protein reader, mediates vancomycin (VAN)-induced AKI.¹⁰ The above finding suggests a role of DNA methylation that is dependent on the specific methylation patterns and type of AKI. Although our previous study has demonstrated that MBD2 promoted AKI induced by VAN,¹⁰ to the date, the role and regulatory mechanisms of MBD2 in septic AKI remain unclear.

In the present study, we demonstrate that MBD2 is induced by lipopolysaccharide (LPS) *in vitro* and *in vivo*. Furthermore, MBD2-knockout (KO) significantly ameliorates septic AKI induced by LPS and cecal ligation and puncture (CLP). Mechanistically, MBD2 mediates LPS-induced expression of protein kinase C η (PKC η) by demethylation of its promoter, resulting in the activation of p38 mitogen-activated protein kinase (MAPK) and extracellular signal-regulated kinase (ERK)1/2 to stimulate renal cell apoptosis and inflammation, respectively. Collectively, these data indicate that MBD2 mediates septic AKI via activation of PKC η /p38MAPK and the ERK1/2 axis.

Received 17 June 2020; accepted 23 September 2020;
<https://doi.org/10.1016/j.omtn.2020.09.028>.

⁸These authors contributed equally to this work.

Correspondence: Dongshan Zhang, Department of Emergency Medicine, Emergency Medicine and Difficult Diseases Institute, Department of Nephrology, Second Xiangya Hospital, Central South University, Changsha, Hunan 410011, People's Republic of China.

E-mail: dongshanzhang@csu.edu.cn

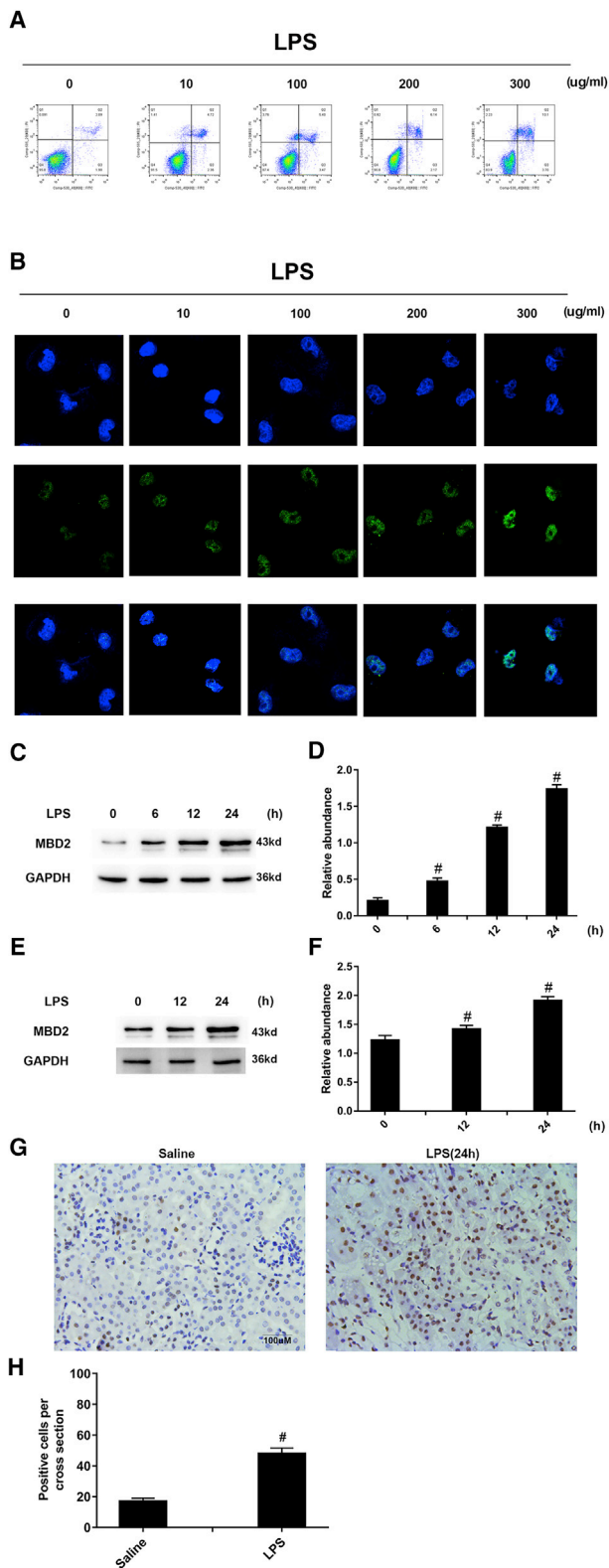


Figure 1. LPS Induced the Expression of MBD-2 in Both BUMPT Cells and Mice Kidneys

BUMPT cells and male C57BL/6 mice were treated with 0–300 µg/mL and 10 mg/kg LPS for 0–24 h, respectively. (A) The FCM analysis of apoptosis. (B) The immunofluorescence detection of MBD2. (C–F) Whole protein lysates from cells and kidneys were gathered for immunoblot analysis of MBD2 and GAPDH expression at the indicated time points (C and E), followed by the densitometric analysis of MBD2 (D and F). (G and H) Immunohistochemical staining (G) and quantitative image analysis (H) of MBD2 expression. Scale bar, 100 µM. Data are expressed as mean ± SD (n = 6). #p < 0.05 versus hour 0 or the saline group. Original magnification, ×200.

RESULTS

Both Apoptosis and MBD2 Were Induced by LPS in BUMPT Cells and C57BL/6 Mice

Although LPS might induce the human kidney proximal tubule (HK-2) cell apoptosis in several cell lines,¹¹ whether it caused Boston University mouse proximal tubule (BUMPT) cell apoptosis remains unclear. The flow cytometry (FCM) analysis results showed that LPS induced the BUMPT cell apoptosis in a dose-dependent manner (0–300 µg/mL) (Figure 1A). Previous studies report that VAN induced expression of MBD2 in HK-2 cells;¹⁰ however, it is unclear whether LPS at 300 µg/mL induces MBD2 expression. In the current study, we demonstrated that LPS induced MBD2 expression in BUMPT cells and C57BL/6 mice for the first time using the immunoblot and immunofluorescence staining (Figures 1B–1F). The immunohistochemistry data further confirm the above finding and indicate that MBD2 is mainly expressed in the nucleus of renal tubular cells (Figures 1F and 1G). Collectively, these data suggest that MBD2 is induced by LPS *in vitro* and *in vivo*.

Attenuation of LPS Induces the Progression of AKI in KO of MBD2 in Mice

To investigate the role of MBD2 in LPS-induced AKI, the MBD2-KO and wild-type (WT) littermate mice were injected with LPS. After LPS treatment, MBD2-KO mice markedly improved the survival rate (Figure 2A). As shown in Figures 2B and 2C, LPS induces impaired renal function in WT mice, as indicated by the elevation of blood urea nitrogen (BUN) and creatinine levels, which were markedly improved in MBD2-KO mice. Interestingly, KO of MBD2 in mice significantly attenuates that LPS caused the increase of serum tumor necrosis factor (TNF)-α and interleukin (IL)-1β (Figures 2D and 2E). Hematoxylin and eosin (H&E) staining indicates that MBD2-KO ameliorated the LPS-induced tubular damage in the cortex and the outer stripe of the outer medulla (OSOM) of the kidney (Figure 2F), which supported the tubular damage scores (Figures 2G and 2H). These results demonstrate that MBD2 mediates LPS-induced progression of AKI.

Attenuation of LPS Induced Renal Cell Apoptosis in MBD-KO Mice

Previous studies have demonstrated that renal cell apoptosis plays a pivotal role in septic AKI;^{12–15} however, the role of MBD2 in LPS-induced AKI is unclear. In the current study, TUNEL staining indicates that LPS increased renal cell apoptosis in the cortex of WT mice, which were reduced in MBD2-KO mice (Figure 3A).

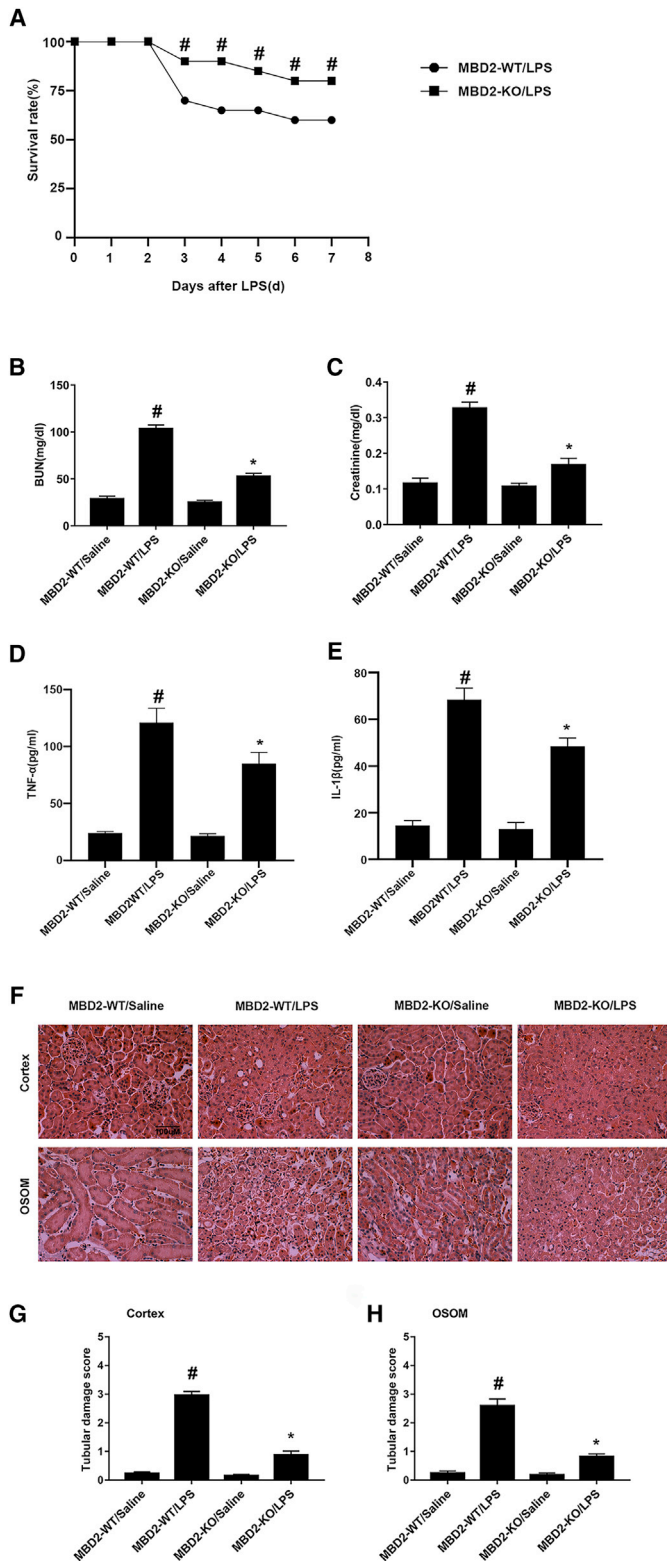


Figure 2. Amelioration of LPS-Induced AKI in MBD2-KO Mice

The MBD2-KO and -WT littermate mice were injected with 10 mg/kg LPS for days 0 to 7 or saline as control. (A) Representative of survival curve. (B and C) Blood samples were collected for the measurement of serum nitrogen (BUN) (B) and creatinine (C) concentration at 24 h. (D and E) Representative of TNF- α (D) and IL-1 β (E). (F) The kidney sections were stained with hematoxylin and eosin (H&E). (G and H) Tubular damage scores of kidney cortex (G) and OSOM (H). Scale bar, 100 μ M. For the survival, the animal number is 12; for other experiments, the data are expressed as mean \pm SD (n = 6). #p < 0.05 versus the saline group; *p < 0.05 versus the MBD2-WT with LPS group. Original magnification, \times 200.

Quantification of TUNEL-positive cells further confirmed the TUNEL staining (Figure 3B). Immunoblot analysis revealed that MBD2-KO markedly suppressed the expression of BAX and cleaved caspase-3 (Figure 3C). These results were supported by gray analysis (Figure 3D). The data suggest that MBD2 is involved in renal cell apoptosis caused by LPS.

The Expression of 54 Genes Was Inhibited during LPS-Induced AKI in MBD2-KO Mice

We hypothesized that MBD2 regulates multiple genes during LPS-induced AKI. LPS induced the upregulation of 4,455 genes in WT mice (Table S1), while downregulating 178 genes in MBD2-KO mice (Table S3). Meanwhile, downregulation of 7,174 genes was induced by LPS in WT mice (Table S2). Interestingly, we found that 54 of 178 downregulated gene promoters exited the CpG island (Figures 4A and 4B), according to the CpG island prediction using the MethPrimer Promoter2.0 (<http://www.urogene.org/cgi-bin/methprimer2/MethPrimer.cgi>). Furthermore, these 54 genes were classified as apoptosis, inflammation, and protein coding (Table 1). Six genes, CRK, Chmp4b, rac1, Csnk1a1, Banp, and PKC η , function in both apoptosis and inflammation. Among these six genes, the fold change of PKC η in LPS versus saline of WT mice is greatest. The real-time polymerase chain reaction (PCR) data confirmed that LPS increases expression levels of PKC η in WT mice, which are significantly suppressed in MBD2-KO mice (Figure 4C). Immunoblot analysis also indicated that MBD2-KO significantly inhibited LPS induction of PKC η and cleaved PKC η (Figures 4D and 4E).

MBD2 Upregulates PKC η Expression by Inhibiting Methylation of the PKC η Promoter

Although MBD2 is involved in PKC η expression, the regulatory mechanism remains unclear. The MethPrimer Promoter2.0 (<http://www.urogene.org/cgi-bin/methprimer2/MethPrimer.cgi>) for CpG island prediction and primer design-based bioinformatics analysis predicted that the promoter of PKC η was located on one island (Figure 5A). As shown in Figure 5B, the chromatin immunoprecipitation (ChIP) assay demonstrated that the immunoprecipitation of MBD2-associated DNA fragments from BUMPT cells contain only one binding site of mBS5, which verified the bioinformatics prediction. Furthermore, the DNA methylation target sequences from the promoter region of PKC η were cloned into the CpG-free pCpGI luciferase reporter plasmid. The MBD2 plasmid markedly enhanced the transcriptional activity compared to the control and mutant plasmids

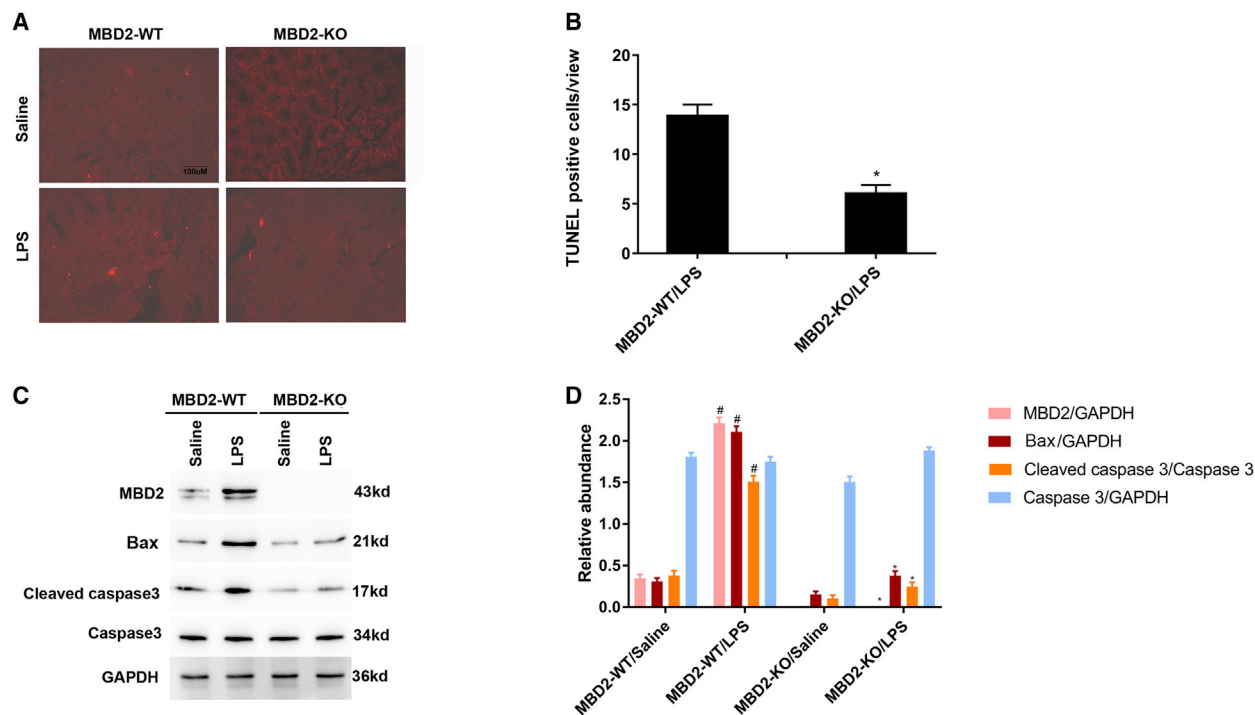


Figure 3. Attenuation of LPS-Induced Renal Cell Apoptosis in MBD2-KO Mice

The MBD2-KO and -WT littermate mice were injected with 10 mg/kg LPS for 24 h or saline as control. (A) TUNEL assay of apoptosis in kidney sections. (B) Quantification of TUNEL-positive cells. (C) Immunoblot analysis of MBD2, BAX, caspase-3, cleaved caspase-3, and GAPDH expression. (D) Grayscale image analysis among them. Scale bar, 100 μ m. Data are expressed as mean \pm SD (n = 6). #p < 0.05 versus the saline group; *p < 0.05 versus the MBD2-WT with LPS group. Original magnification, \times 200.

of MBD2-methylated DNA-binding domain deletion (Figure 5C). Methylation analysis demonstrated that endogenous MBD2-bound DNA markedly suppresses the methylated pCpGI of PKC η , which was enhanced further by ectopic MBD2 expression (Figure 5D). The immunoblot analysis verified that LPS increases the expression levels of both PKC η and cleaved PKC η , which were enhanced by MBD2 overexpression (Figures 5E and 5F) and reduced by MBD2 small interfering RNA (siRNA) treatment (Figures 5G and 5H). These data suggest that MBD2 upregulates the expression of PKC η via promoter demethylation.

MBD2-Mediated LPS Induced the BUMPT Cell Apoptosis

To further confirm the *in vivo* findings of LPS-induced renal cell apoptosis, BUMPT cells were transfected with MBD2 or MBD2 siRNA, with or without LPS. As shown in Figure 6A, the results of FCM analysis demonstrate that LPS increases the apoptosis ratio of BUMPT cells, which were enhanced by the expression of MBD2 (Figure 6A). Immunoblot analysis indicates that LPS upregulates the expression of MBD2, BAX, and cleaved caspase-3, which are further enhanced by MBD2 overexpression (Figure 6B). The gray analysis result confirmed the changes of these proteins (Figure 6C). In contrast, MBD2 siRNA markedly attenuates LPS-stimulated apoptosis in BUMPT cells (Figure 6D) and the expression of MBD2, BAX, and cleaved caspase-3 (Figures 6E and 6F). Collectively, these data confirm that MBD2 is involved in LPS-induced BUMPT cell apoptosis.

MBD2 Is Involved in the Expression of TNF- α , IL-1 β , and ICAM1 Caused by LPS in BUMPTs

Since inflammation plays an important role in LPS-induced AKI,¹⁶ we want to investigate whether MBD2 mediates LPS-induced inflammation. As shown in Figure 7A, LPS increases the expression of TNF- α , IL-1 β , and ICAM1 in BUMPT cells, which were further upregulated by MBD2 expression; this was further verified by the immunoblot of them (Figures 7B and 7C). By contrast, MBD2 siRNA markedly reduces the expression of TNF- α , IL-1 β , and ICAM1 stimulated by LPS in BUMPT cells (Figure 7D), which were confirmed by the immunoblot of them (Figures 7E and 7F). Furthermore, the primary renal tubular epithelial cells from MBD2-KO mice ameliorated the LPS-induced expression of TNF- α , IL-1 β , and ICAM1 (Figures 7G and 7H). However, the M0 (nonactivated macrophage) macrophages came from transition of the primary murine bone marrow-derived monocytes of the MBD2-KO mice and only attenuated the LPS-induced expression of TNF- α but did not affect the downregulation of IL-1 β and ICAM1 (Figures 7I and 7J). These results verify that MBD2 mediates LPS-induced expression of inflammatory factors.

PKC η siRNA Suppresses LPS-Induced Renal Cell Apoptosis in BUMPT Cells via Inactivation of p38MAPK

To date, the role and regulation of PKC η during LPS-induced BUMPT cell apoptosis remain unclear. FCM analysis verified that PKC η siRNA notably suppresses BUMPT cell apoptosis (Figure 8A).

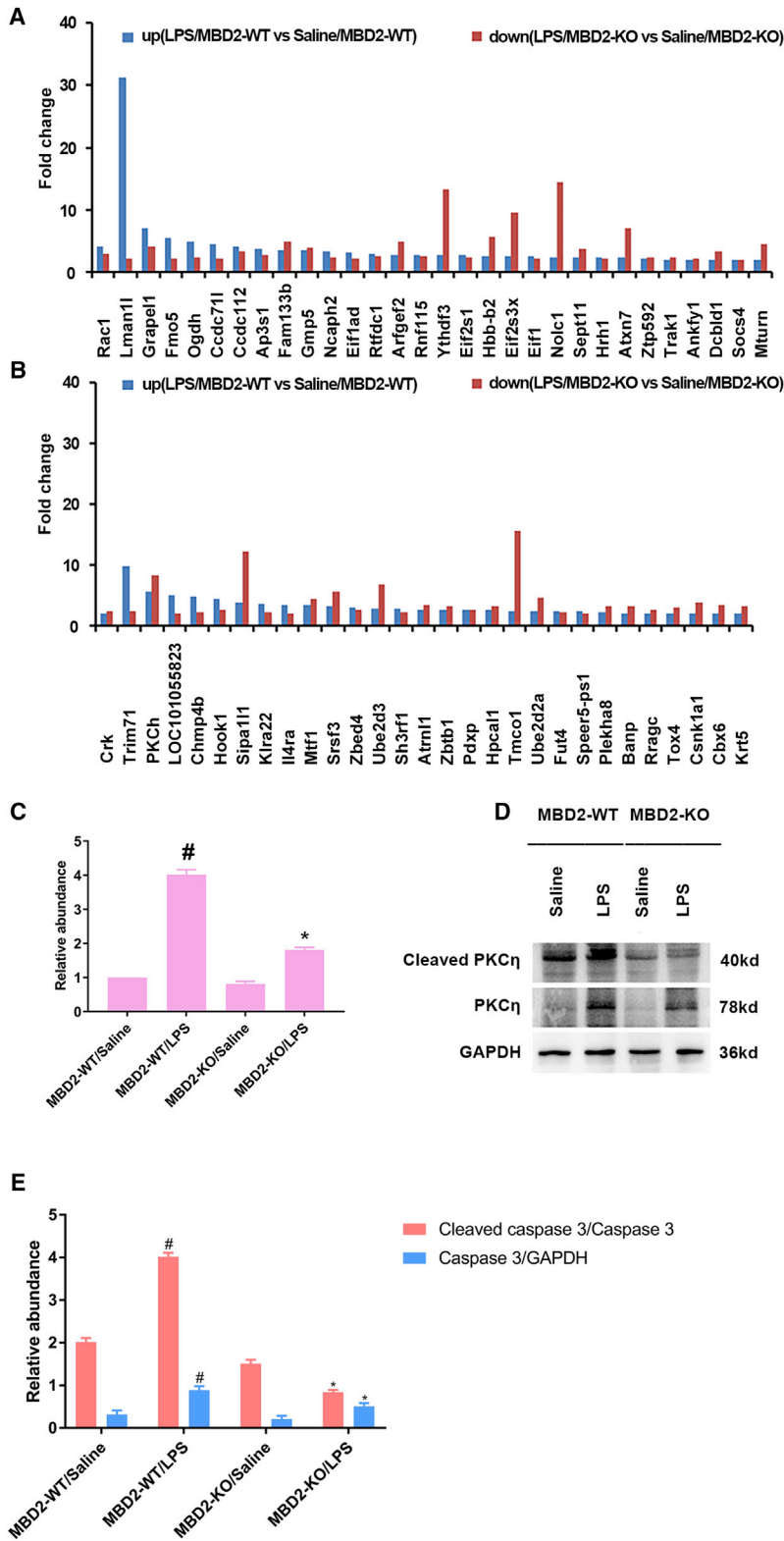


Figure 4. The Induction of PKC η during LPS-Induced AKI is Inhibited in MBD2-KO Mice

The MBD2-KO and -WT littermate mice were injected with 10 mg/kg LPS for 24 h or saline as control. (A) The amount of 30 genes from the LPS group was divided by the amount of saline control to calculate the fold change. (B) The amount of 29 genes from the LPS group was divided by the amount of saline control to calculate the fold change. (C) Real-time PCR analysis of PKC η expression. (D) Immunoblot analysis of PKC η , cleaved PKC η , and GAPDH expression. (E) Grayscale image analysis between them. Data are expressed as mean \pm SD (n = 6). #p < 0.05 versus the saline group; *p < 0.05 versus the MBD2-WT with LPS group.

Table 1. Fifty-Four Genes Induced by MBD2 during LPS-Induced AKI

Gene Function	Gene Name
Apoptosis	TRIMI71/CRK/OGDH/Chmp4b/rac1/MTF1/SRSF3/Ube2d3/Sh3rt1/Zbxb1/Eif2s1/Hpcal1/NOLF1/Fut4/Plekha8/Atxn7/PRKCH/Banp/Tox4/Csnk1a1
	CRK/fom5/Chmp4b/rac1/Il4ra/RNF115/Zbtb1/Hrh1/PRKCH/Banp/Csnk1a1/Socs4
Inflammation	Lman11/Grpel1/Ccdc711/Hook1/Ccdc112/Ap3s1/Fam133b/Gmps/Ncaph2/Rtfdc1/Arfg
	e2/Atml1/Ythdf3/Eif2s3x/Tmco1/eif1/Sept11/Zfp592/Rragc/Trak1/Trim23/Ankfy1/D
Protein coding	cblld1/Cbx6/Kft5/Mturn
	Sipa111/PDXP/Speer5-ps1
Unknown	

Immunoblot analysis reveals that LPS increased the expression of MBD2, BAX, and cleaved caspase-3, which were markedly inhibited by the PKC η siRNA, with the exception of MBD2 (Figure 8B). These changes were verified by gray analysis (Figure 8C). As shown in Figure 8D, immunoblot analysis revealed that LPS increases the expression of PKC η , cleaved PKC η , and phosphorylated (p)-p38MAPK, which were markedly suppressed by the PKC η siRNA. Gray analysis confirmed the expression changes in these proteins (Figure 8E). Furthermore, FAM analysis indicates that inactivation of p38MAPK using SB203580 attenuates LPS-induced BUMPT cell apoptosis (Figure 8F). The immunoblot analysis also confirmed that SB203580 markedly suppressed the activation of p38MAPK (Figures 8G and 8H). To confirm whether p38MAPK mediated the promoting apoptosis role of PKC η during LPS treatment, the p38MAPK activator was used in the current study. The FCM analysis indicated that the p38MAPK activator completely reversed the effect of PKC η siRNA on LPS-induced BUMPT cells apoptosis (Figure 8I), which was further verified by the immunoblot analysis (Figures 8J and 8K). These data suggest that PKC η mediates LPS-induced BUMPT cell apoptosis via activation of p38MAPK.

PKC η siRNA Suppresses LPS-Induced Expression of COX2, iNOS, TNF- α , IL-1 β , and ICAM1 in BUMPT Cells via Inactivation of ERK1/2

A previous study has reported that PKC η activates the inflammatory signal pathway¹⁷, and ERK1/2 signaling is involved in LPS induced expression of COX2 and inducible nitric oxide synthase (iNOS).¹⁸ Hence, we hypothesized that PKC η mediates LPS-induced inflammation via inactivation of ERK1/2 signaling. As shown in Figure S1A, immunoblot analysis results indicate that PKC η siRNA markedly suppresses LPS-induced expression of p-ERK1/2, COX2, and iNOS, which were confirmed by gray analysis (Figure S1B). Furthermore, real-time PCR analysis indicates that PKC η siRNA notably suppresses the expression of TNF- α , IL-1 β , and ICAM1 caused by LPS in BUMPT cells (Figure S1C), which were further confirmed by the immunoblot of them (Figures S1D and S1E). Furthermore, we also demonstrated that inhibition of ERK1/2 also attenuated the LPS-

induced the expression of TNF- α , IL-1 β , ICAM1, COX2, and iNOS (Figures S1F and S1G). To confirm if ERK1/2 mediated the promoting inflammation role of PKC η during LPS treatment, the ERK1/2 activator was applied. The immunoblot analysis demonstrated that the ERK1/2 activator almost reversed the effect of PKC η siRNA on LPS-induced production of TNF- α , IL-1 β , ICAM1, COX2, and iNOS (Figure S1H), which were further verified by the gray analysis (Figure S1I). These data suggest that PKC η /ERK1/2 signaling mediates LPS-induced inflammation.

PKC η Mediated the Effect of MBD2 on LPS-Induced Apoptosis and Inflammation

To further demonstrate if PKC η mediated the role of MBD2 during LPS treatment, we designed the two experiments. First, the FCM analysis demonstrated that overexpression of PKC η notably reversed the effect of MBD2 siRNA on LPS-induced apoptosis (Figures S2A). The immunoblot analysis further confirmed that overexpression of PKC η markedly reversed the effect of MBD2 siRNA on LPS-induced expression of BAX, caspase-3, and cleaved caspase-3, TNF- α , IL-1 β , ICAM1, COX2, and iNOS (Figures S2B and S2C). In addition, overexpression of MBD2 did not attenuate the effect of the PKC η siRNA on LPS-induced apoptosis, apoptosis-associated genes, and inflammation-associated genes (Figures S2D–S2F). Taken together, the data further confirmed that PKC η was a direct downstream of MBD2.

PKC η siRNA Suppresses CLP-Induced AKI in C57BL/6 Mice

To investigate the role of PKC η in CLP-induced AKI, C57BL/6 mice were subjected to CLP and then treated with PKC η siRNA. After CLP treatment, PKC η siRNA markedly improved the survival rate (Figure S3A). As shown in Figures S3B and S3C, CLP induces impaired renal function in C57BL/6 mice, as indicated by the elevation of BUN and creatinine levels, which were markedly improved in PKC η siRNA. Interestingly, PKC η siRNA significantly attenuates that CLP caused the increase of serum TNF- α and IL-1 β (Figures S3D and S3E). The result of H&E staining demonstrated that PKC η siRNA treatment reduces CLP-induced tubular damage in the cortex and OSOM of kidney (Figure S3F). Tubular damage scores confirmed the H&E staining results (Figures S3G and S3H). These data suggest that PKC η is involved in CLP-induced AKI.

PKC η siRNA Suppresses Renal Cell Apoptosis and Inflammation by Inactivation of p38MAPK and ERK1/2

To further confirm the *in vitro* regulatory mechanism of PKC η , mice were subjected to CLP and then treated with PKC η siRNA. TUNEL staining indicates that PKC η siRNA treatment markedly attenuates renal cell apoptosis in the cortex of C57BL/6 mice, which are suppressed by PKC η siRNA (Figure S4A). This was confirmed by the quantification of TUNEL-positive cells (Figure S4B). Immunoblot revealed that PKC η siRNA notably suppresses CLP-induced expression of cleaved PKC η , BAX, cleaved caspase-3, p-p38MAPK, p-ERK1/2, iNOS, and COX2 (Figure S4C), which were verified by gray analysis (Figures S4D and S4E). Finally, PCR and immunoblot analysis further confirmed that CLP induces the expression of TNF- α , IL-1, and ICAM1, which are inhibited by PKC η siRNA (Figures S5A–S5C).

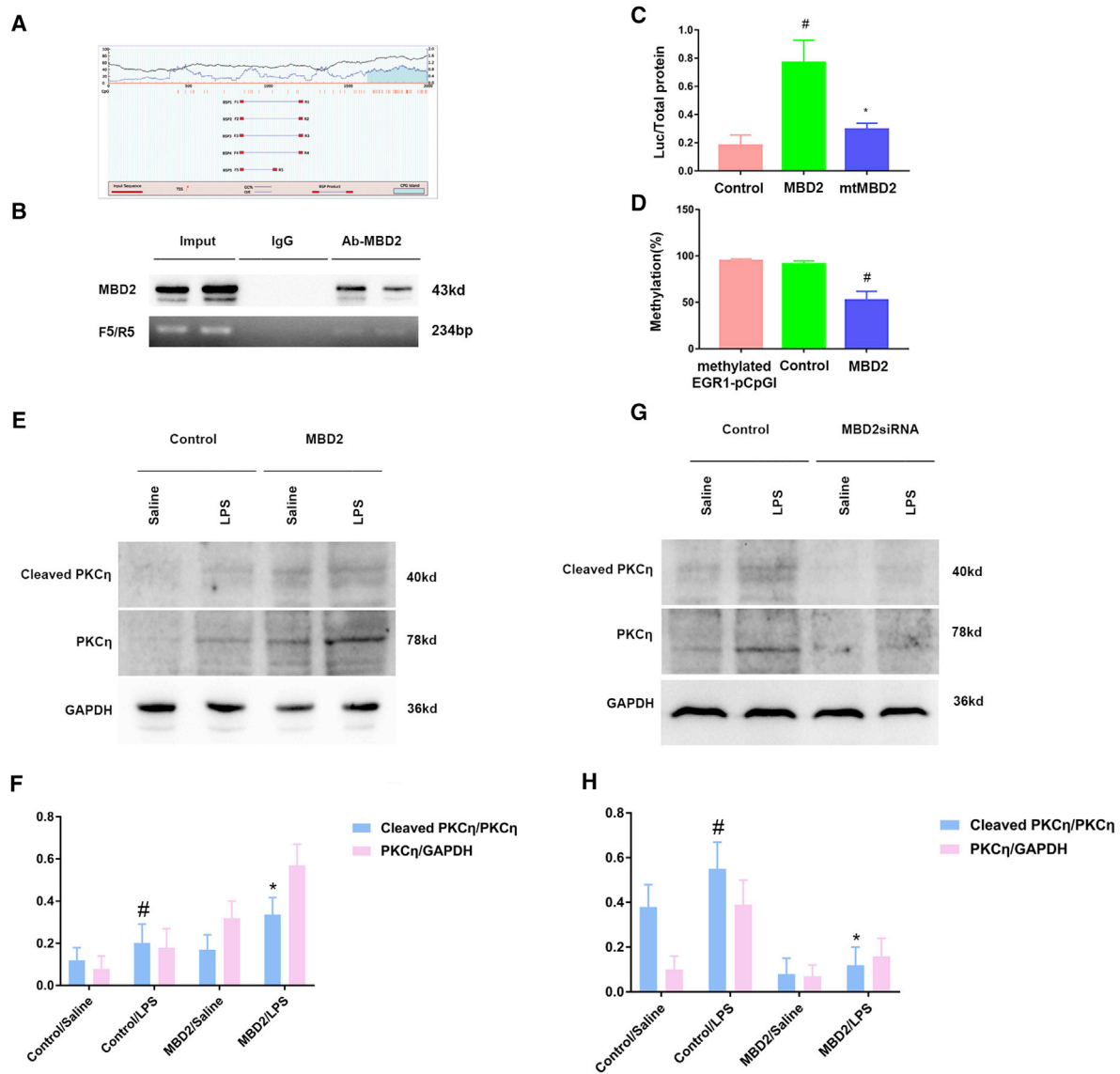


Figure 5. MBD2 Directly Binds to CpG Islands of Promoter of PKC η and Positively Activates Transcription of Them by Hypomethylation of the Promoter

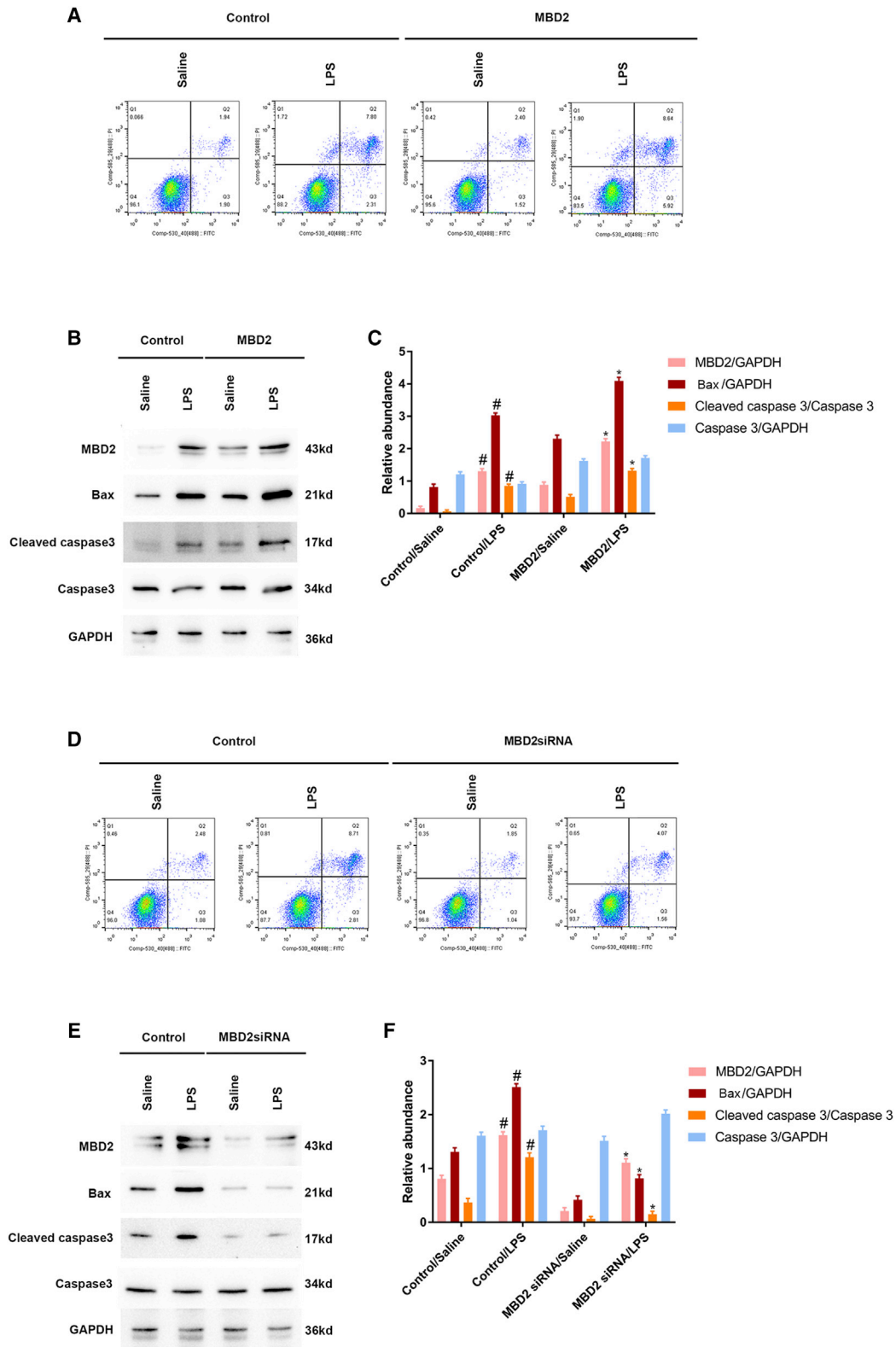
(A) The patterns of CpG islands of the PKC η promoter and five pairs of the primer were predicted by the software of MethPrimer Promoter2.0. (B) ChIP assays represent the binding sites of MBD2 interaction with CpG islands of the promoter of PKC η . (C) Relative luciferase activity of MBD2 or MBD2 mutation plasmids cotransfected with the methylated PKC η pCpG plasmid in BUMPT cells. (D) CpG-DNA methylation of the PKC η promoter region. (E) Immunoblot analysis of PKC η , cleaved PKC η , and GAPDH expression after LPS treatment with or without transfection of MBD2. (F) Grayscale image analysis between them after LPS treatment with or without transfection of MBD2. (G) Immunoblot analysis of PKC η , cleaved PKC η , and GAPDH expression after LPS treatment with or without transfection of MBD2 siRNA. (H) Grayscale image analysis between them after LPS treatment with or without transfection of MBD2 siRNA. These data are representative of at least four separate experiments shown as means \pm SD (n = 6). #p < 0.05 versus the control group; *p < 0.05 versus the MBD2 plasmid or LPS group.

These data provide strong evidence that PKC η mediates CLP-induced renal cell apoptosis and inflammation via activation of p38MAPK and ERK1/2.

Attenuation of CLP-Induced AKI in MBD2-KO Mice

To confirm the role of MBD2 in septic AKI, the MBD2-KO and -WT littermate mice were subjected to CLP. After CLP treatment, MBD2-

KO markedly improved the survival rate (Figure S6A). As shown in Figures S3B and S3C, CLP induced the elevation of BUN and creatinine concentration in WT mice, which are reduced in MBD2-KO mice (Figures S6B and S6C). MBD2-KO significantly attenuated the CLP, which caused the increase of serum TNF- α and IL-1 β (Figures S6D and S6E). H&E staining indicates that MBD2-KO ameliorates CLP-induced tubular damage in the cortex and OSOM of kidney



(legend on next page)

(Figure S6F), which was verified by the tubular damage scores (Figures S6G and S6H). These data further confirm the role of MBD2 in septic AKI.

Amelioration of CLP-Induced Renal Cell Apoptosis and Inflammation by Inactivation of PKC η /p38MAPK and the ERK1/2 Axis

To confirm the regulatory mechanism of MBD2 for septic AKI, MBD2-KO and -WT littermate mice were subjected to CLP for 18 h. As shown in Figure S7A, TUNEL staining indicated that MBD2-KO reduced renal cell apoptosis in the cortex of C57BL/6 mice. The quantification of TUNEL-positive cells verified the TUNEL staining data (Figure S7B). Immunoblot analysis indicates that CLP induced the expression of MBD2, BAX, cleaved caspase-3, cleaved PKC η , p-p38MAPK, p-ERK1/2, iNOS, and COX2 (Figures S7C and S7E). Gray analysis confirmed the expression-level changes of these proteins (Figures S7D, S7F, and S7G). Finally, the real-time PCR and immunoblot analysis indicated that MBD2-KO reduced CLP-induced expression of TNF- α , IL-1 β , and ICAM1 (Figures S8A–S8C). These data suggest that MBD2/PKC η /p38MAPK and the ERK1/2 axis mediate renal cell apoptosis and inflammation during CLP-induced AKI.

DISCUSSION

Our previous studies have demonstrated that MBD2 is involved in AKI-associated VAN;¹⁰ however, the role of MBD2 in septic AKI was unclear. In the present study, we initially found that MBD2 mediates LPS- and CLP-induced AKI. Next, a gene chip assay revealed that six genes involved in apoptosis and inflammation were upregulated in LPS-AKI via MBD2. Finally, MBD2/PKC η /p38MAPK and the ERK1/2 signaling axis mediate renal cell apoptosis and inflammation during septic AKI (Figure S9).

A previous study indicated that MBD2 is induced by VAN.¹⁰ In the current study, we report that MBD2 is also stimulated by LPS *in vitro* and *vivo*, mostly expressed in the nuclei of injured tubular cells (Figure 1). To investigate the role of MBD2 in septic AKI, MBD2-KO mice were used in the current study. The results indicate that MBD2-KO ameliorates both LPS- and CLP-induced AKI and improved the survival rate (Figures 2 and S6). Recent studies have recognized that apoptosis plays a crucial role in septic AKI.^{14,19} Our study verified that MBD2 is involved in renal cell apoptosis, which is demonstrated by TUNEL staining (Figures 3A, 3B, S7A, and S7B), the immunoblot of BAX and cleaved caspase 3 (Figures 3C, 3D, S7C, and S7D), and the overexpression of MBD2 or MBD2 siRNA (Figure 6). Interestingly, the quantification of TUNEL-positive

cells suggests that the amount of apoptosis in LPS-induced AKI is less than in the CLP-induced AKI model, possibly explaining differences in severity of sepsis models. In addition, we also found that the LPS-induced production of TNF- α , IL-1, and ICAM1 was inhibited by the MBD2 siRNA or MBD2-KO and by contrast, reinforced by MBD2 overexpression (Figures 7A–7H); however, MBD2-KO-only LPS or CLP induced the production of TNF- α but not IL-1 and ICAM1 in primary M0 macrophages (Figures 7I, 7J, and S8). The difference may be due to inconsistencies in the response of primary tubular epithelial cells and macrophages to LPS. These findings are consistent with a previous study in which MBD2 mediated renal cell apoptosis and inflammation induced by VAN.¹⁰

To further investigate the molecular mechanism of how MBD2 mediates LPS-induced apoptosis and inflammation, a gene chip assay was used to assess gene expression. Following LPS treatment, the expression of PKC η was positively regulated by the MBD *in vivo* and *in vitro* (Figures 4 and 5E–5H). Mechanistically, MBD2 induced the expression of PKC η via the suppression of methylation (Figures 5B–5D). MBD2 siRNA attenuated the LPS-induced BUMPT cell apoptosis; upregulation of BAX and cleaved caspase-3; and production of TNF- α , IL-1 β , ICAM1, iNOS, and COX2. Interestingly, this was markedly reversed by PKC η overexpression (Figures S2A–S2C). Although PKC η siRNA also ameliorated the above effect of LPS, this was not affected by MBD2 overexpression (Figures S2D–S2F). The data indicated that PKC η was a directly downstream of MBD2.

Recent studies suggest that PKC η is induced by LPS in primary astrocytes.²⁰ However, the role of PKC η in apoptosis remains controversial. Some studies report that PKC η protects against apoptosis in several cell lines.^{21,22} In contrast, one study reported that PKC η promotes high glucose (HG)-induced apoptosis in HK-2 cells.²³ The FAM analysis indicated that PKC η mediates LPS-induced BUMPT cell apoptosis (Figure 8A), which was confirmed by immunoblot analysis of BAX and cleaved caspase-3 (Figures 8B and 8C). To further explore the signaling mechanism of PKC η -mediated apoptosis, we assessed the expression of p-p38MAPK. An immunoblot assay demonstrated that inhibition of PKC η markedly suppressed the activation of p38MAPK (Figures 8D and 8E). Furthermore, inactivation of p38MAPK notably suppressed BUMPT cell apoptosis (Figures 8F–8H), which is supported by the observation that inhibition of p38MAPK reduced TNF- α or albumin-induced podocyte apoptosis.^{24–26} Interestingly, the effect of PKC η siRNA on LPS-induced apoptosis and associated gene expression was reversed by the activator of p38MAPK, which suggested that p38MAPK was one of the downstream signal pathways of PKC η (Figures 8I–8K).

Figure 6. MBD2-Mediated LPS Induced Renal Cell Apoptosis in BUMPT Cells

(A) The FCM analysis of apoptosis after LPS treatment with or without transfection of MBD2. (B) Immunoblot analysis of MBD2, BAX, caspase-3, cleaved caspase-3, and GAPDH expression after LPS treatment with or without transfection of MBD2. (C) The proteins signal was quantified by densitometry and normalized to internal control of GAPDH after LPS treatment with or without transfection of MBD2. (D) The FCM analysis of apoptosis after LPS treatment with or without transfection of MBD2 siRNA. (E) Immunoblot analysis of MBD2, BAX, caspase-3, cleaved caspase-3, and GAPDH expression after LPS treatment with or without transfection of MBD2 siRNA. (F) The proteins signal was quantified by densitometry and normalized to internal control of GAPDH after LPS treatment with or without transfection of MBD2 siRNA. Data are expressed as mean \pm SD (n = 6). #p < 0.05 versus the saline group; *p < 0.05 versus the MBD2 plasmid or MBD2 siRNA with LPS group.

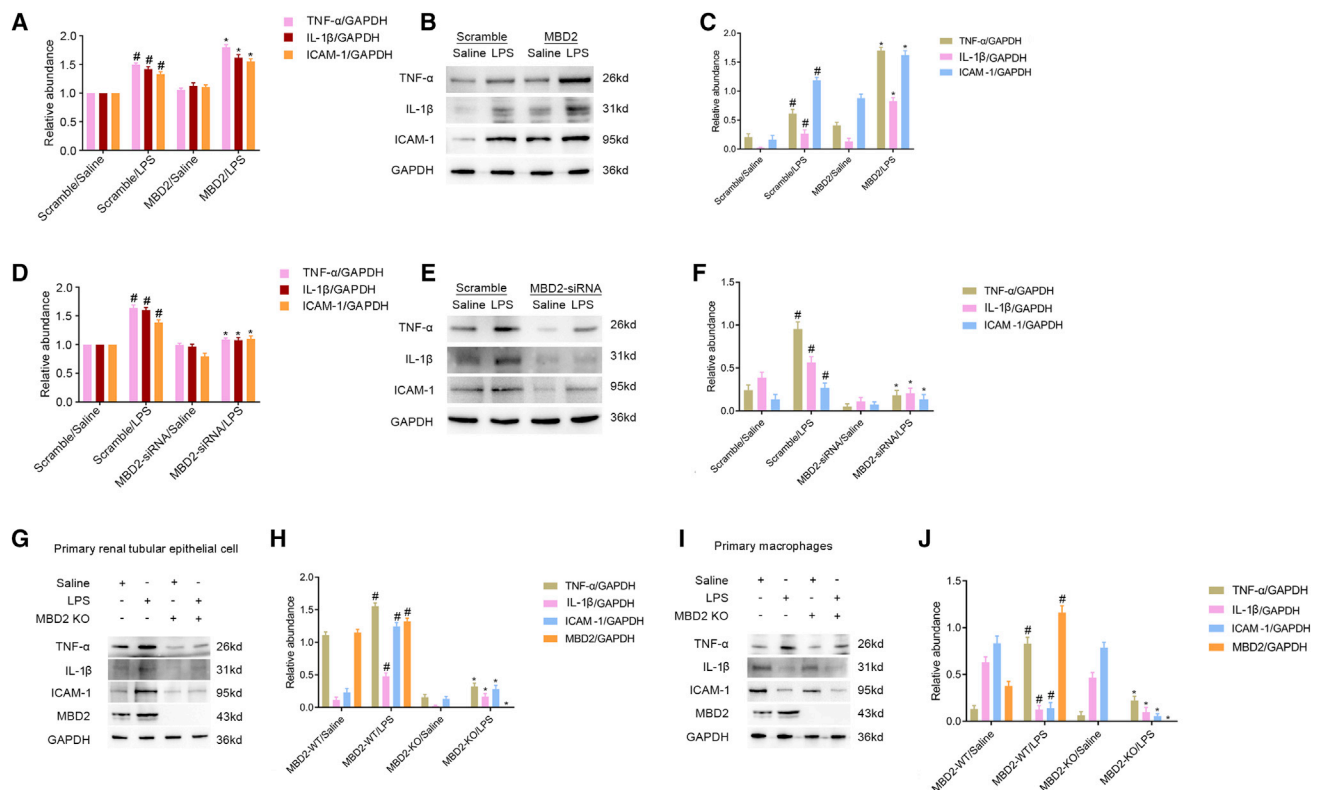


Figure 7. MBD2-Mediated LPS Induced the Expression of TNF- α , IL-1 β , and ICAM1 in BUMPT Cells

BUMPT cells were transfected with MBD2 plasmid or MBD2 siRNA or primary macrophages from bone marrow of MBD2 and MBD2-KO mice, followed by treatment with 300 μ g/mL LPS for 24 h. (A) Real-time PCR analysis of TNF- α , IL-1 β , and ICAM1 expression after LPS treatment with or without transfection of MBD2. (B) Immunoblot analysis of TNF- α , IL-1 β , ICAM1, or MBD2, and GAPDH after LPS treatment with or without transfection of MBD2. (C) The protein signal was quantified by densitometry and normalized to internal control of GAPDH after LPS treatment with or without transfection of MBD2. (D) Real-time PCR analysis of TNF- α , IL-1 β , and ICAM1 expression after LPS treatment with or without transfection of MBD2 siRNA. (E) Immunoblot analysis of TNF- α , IL-1 β , ICAM1, or MBD2, and GAPDH after LPS treatment with or without transfection of MBD2 siRNA. (F) The protein signal was quantified by densitometry and normalized to internal control of GAPDH after LPS treatment with or without transfection of MBD2 siRNA. (G) Immunoblot analysis of TNF- α , IL-1 β , ICAM1, or MBD2, and GAPDH in MBD2 KO primary tubular cells with LPS treatment. (H) The protein signal was quantified by densitometry and normalized to internal control of GAPDH in MBD2 KO primary tubular cells with LPS treatment. (I) Immunoblot analysis of TNF- α , IL-1 β , ICAM1, or MBD2, and GAPDH in MBD2 KO primary macrophage cells with LPS treatment. (J) The protein signal was quantified by densitometry and normalized to internal control of GAPDH in MBD2 KO primary macrophage cells with LPS treatment. Data are expressed as mean \pm SD (n = 6). #p < 0.05 versus the saline group; *p < 0.05 versus the MBD2 plasmid or MBD2 siRNA with LPS group; Δ p > 0.05 versus the LPS group.

In addition, our previous study reported that ERK1/2 mediates LPS-induced expression of COX2 and iNOS.¹⁸ In the present study, we demonstrated that knockdown of PKC η suppresses the expression of p-ERK1/2, which is accompanied by the downregulation of COX2, iNOS, TNF- α , IL-1, and ICAM1; by contrast, the effect of PKC η siRNA on LPS-induced inflammation-associated gene expression was also reversed by the activator of ERK1/2 (Figure S1), suggesting that ERK1/2 was one of the downstream signal pathways of PKC η . Finally, inhibition of PKC η attenuates CLP-induced AKI, renal cell apoptosis, inflammation via inactivation of p38MAPK, and ERK1/2 signaling and improved survival rate (Figures S3 and 4). Collectively, these data suggest that PKC η /p38MAPK and the ERK1/2 axis mediate LPS-induced apoptosis and inflammation *in vitro* and *in vivo*, which was further confirmed in CLP-induced AKI using MBD2-KO mice (Figures S7E–S7G).

In summary, our data verify that MBD2 is involved in septic AKI induced by LPS and CLP. Furthermore, MBD2 induces the expression of PKC η via promoter hypomethylation, subsequently activating p38MAPK and ERK1/2 signaling pathways to induce renal cell apoptosis and inflammation during septic AKI, respectively. The data indicate that MBD2 is a potential therapeutic target for septic AKI.

MATERIALS AND METHODS

Reagents and Antibodies

Antibodies were obtained from multiple sources: glyceraldehyde 3-phosphate dehydrogenase (GAPDH) and β -actin were from Santa Cruz Biotechnology (Santa Cruz, CA, USA); MBD2 and PKC η were from Abcam (Cambridge, MA, USA); caspase-3, cleaved caspase-3, p-ERK1/2, ERK1/2, p-p38MAPK, p38MAPK, COX-2, and iNOS were from Cell Signaling Technology (Dancers, MA, USA).

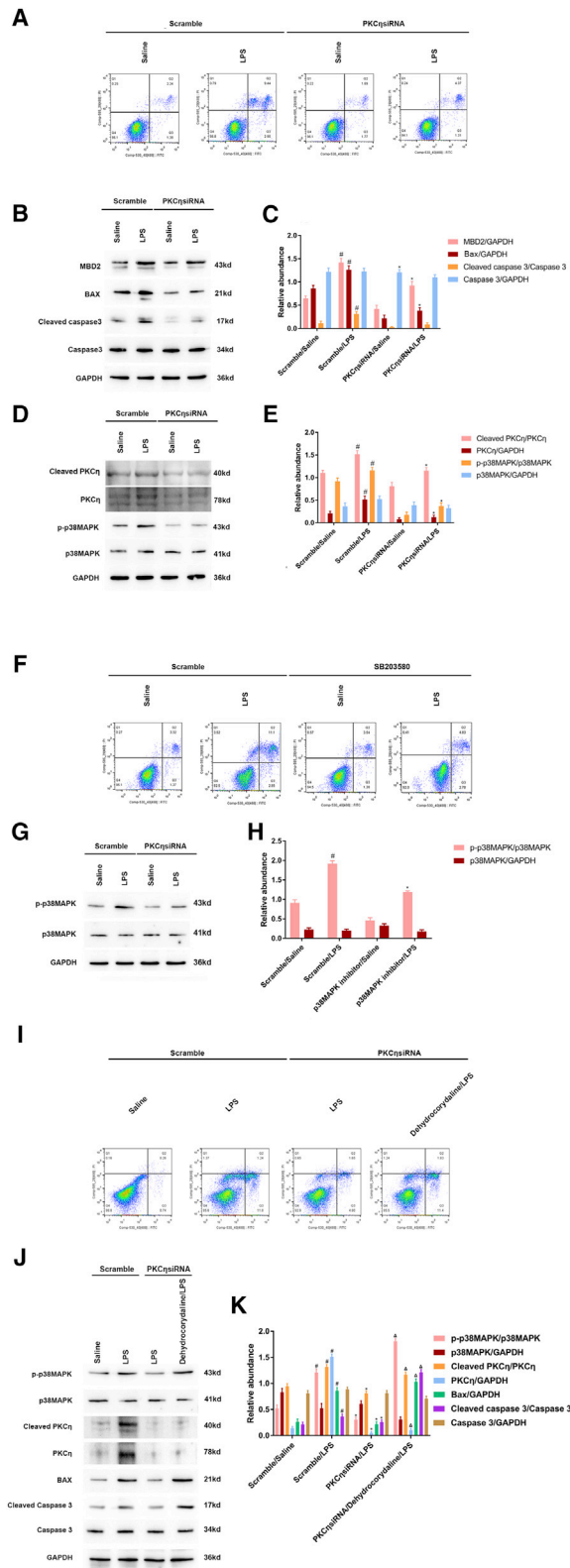


Figure 8. PKC η Mediated LPS-Induced Renal Cell Apoptosis and the Expression of BAX and Cleaved Caspase-3 in BUMPT Cells via Activation of p38MAPK

BUMPT cells were used the p38MAPK inhibitor (SB203580) or transfected with PKC η siRNA plus with or without the p38MAPK activator (dehydrocorydaline chloride) or and then followed by treatment with 300 μ g/mL LPS for 24 h. (A) FCM analysis of apoptosis. (B) Immunoblot analysis of MBD2, BAX, caspase-3, cleaved caspase-3, and GAPDH expression. (C) Grayscale image analysis among them. (D) Immunoblot analysis of PKC η , cleaved PKC η , p38MAPK, and p-p38MAPK expression. (E) Grayscale image analysis among them. (F) FCM analysis of apoptosis. (G) Immunoblot analysis of p38MAPK and p-p38MAPK expression. (H) Grayscale image analysis between them. (I) FCM analysis of apoptosis. (J) Immunoblot analysis of p38MAPK, p-p38MAPK PKC η , cleaved PKC η , BAX, caspase-3, cleaved caspase-3, and GAPDH. (K) Grayscale image analysis among them. Data are expressed as mean \pm SD (n = 6). #p < 0.05 versus the scramble with saline group; *p < 0.05 versus the scramble with LPS group; Δ p > 0.05 versus the scramble with LPS group.

TNF- α , IL-1 β , and ICAM1 are from Proteintech North America (Rosemont, IL, USA). p38MAPK activator dehydrocorydaline chloride and pERK1/2 activator honokiol were purchased from MedChemExpress USA (Deer Park, NJ, USA). LPS was obtained from Sigma (St. Louis, MO, USA). The methylation promoter PKC η was subcloned into a CpG-free pCpGI luciferase reporter vector by Invitrogen Biotechnology (Shanghai, China). The plasmids of MBD2, mtMBD2 lacking the methylated DNA binding domain, and PKC η were constructed by the Ruqi biology company (Guangdong, Guangzhou, China). siRNAs against MBD2 and PKC η were synthesized by the Ruibo biology company (Guangdong, Guangzhou, China), as previously described.¹⁰

Animal Model

MBD2-KO mice were obtained from Cyagen Biosciences (Guangzhou, People’s Republic of China). The littermate mice of MBD2-WT and MBD2-KO (male, aged 10–12 weeks) were injected intraperitoneally with LPS at 10 mg/kg, whereas the control group was administered normal saline. The littermate mice of MBD2-WT and MBD2-KO (male, aged 10–12 weeks) were also subjected to CLP to induce AKI, as previously described.¹⁸ The mice (male, aged 10–12 weeks) were injected intraperitoneally with LPS at 10 mg/kg or subjected to CLP and then injected intraperitoneally with PKC η siRNA (15 mg/kg) 1 h after CLP treatment. The control group was administered normal saline. Renal tissues were harvested for various biochemical and morphologic analyses at 24 h following LPS or at 18 h after CLP. Animal experiments were carried out in strict accordance with the guide by the Institutional Committee for the Care and Use of Laboratory Animals of Second Xiangya Hospital, China. All animals were housed on a 12-hour light/dark cycle and were allowed free access to food and water.

Cell Culture and Treatments

BUMPT cells were cultured in Dulbecco’s modified Eagle’s medium with 10% fetal bovine serum, 0.5% penicillin (Thermo Fisher Scientific), and streptomycin and then maintained in a 5% CO₂ incubator at 37°C. After 24 h transfection of MBD2 siRNA or PKC η siRNA or negative control or MBD2 plasmid, the BUMPT cells were treated with 300 μ g/mL LPS for 24 h.

The Analysis of ChIP and Transcriptional Activation Activity

The ChIP experiment was carried out using anti-MBD2, according to the procedure of the ChIP kit (Millipore, USA).^{10,27–31} Immunoprecipitated DNAs were amplified by PCR with primers of CpG islands' binding of promoter of PKC η : forward (F)1: 5'-TTAAATTATGTGTTAGAAAGGGGA-3', reverse (R)1: 5'-ACAAAACCAAAATATAATAATCCCTTC-3'; F2: 5'-TTAAATTATGTGTTAGAAAGGGGA-3', R2: 5'-CAAAACCAAAATATAATAATCCCTTC-3'; F3: 5'-GTAAATTATGTGTTAGAAAGGGGA-3', R3: 5'-ACAAAACCAAAATATAATAATCCCTTC-3'; F4: 5'-GTAAATTATGTGTTAGAAAGGGGA-3', R4: 5'-CAAAACCAAAATATAATAATCCCTTC-3'; F5: 5'-TTAAATTATGTGTTAGAAAGGGGA-3', R5: 5'-AAATAAACAAACCCTAAATTTACCCAT-3'. The relative activity of the luciferase kit (Promega) was used to detect the transcriptional activation activity of PKC η , as previously described.¹⁰

Methylated CpG-DNA Immunoprecipitation (MCIP)

The MCIP was performed as previously described (Zymo Research).³² Briefly, sheared DNA was used for MCIP, and then methylated DNA was analyzed by PCR analysis using an Applied Biosystems StepOne-Plus Real-Time PCR System.

Histology, Immunohistochemistry, and Immunoblot Analyses

Histological analysis involved H&E staining. The percentage of damaged tubules was used to assess the score of tissue damage: 0, no damage; 1, <25% damage; 2, 25%–50% damage; 3, 51%–75% damage; 4, >75% damage. The criteria of tubular damage contained brush border, the loss of tubular dilation, tcast formation, and cell lysis.^{10,33} The TUNEL kit was used for renal cell apoptosis and then quantified by calculating the percentage of total number of TUNEL-positive cells in 10–20 microscopic fields per tissue section.³³ Immunohistochemical analyses were carried out by using antibodies of MBD2 and F4/80 and quantified as previously described.³⁴ For immunoblot analysis, tissue lysates of kidneys and BUMPT cells were collected to SDS-PAGE electrophoresis and immunoblotted with antibody of MBD2, PKC η , cspase-3, cleaved caspase-3, p-ERK1/2, ERK1/2, p-p38MAPK, p38MAPK, COX-2, and iNOS following standard procedures.

Real-Time PCR

Quantitative real-time RT-PCR amplifications were performed as previously described.^{30,35,36} The following primer pairs were used: TNF- α : F: 5'-TAGCCAGGAGGGAGAACAGA-3', R: 5'-TTTTCTGGAGGGAGATGTGG-3'; ICAM-1: F: 5'-CTTCCAGCTACCATCCAAA-3', R: 5'-CTTCAGAGGCAGGAAACAGG-3'; IL-1: F: 5'-CTCGTGCTGTCGGACCCATA-3', R: 5'-CAGGCTTGTGCTCTGCTTGTGA-3'; GAPDH: F: 5'-CGTCCCGTAGACAAAATGGT-3', R: 5'-TTGATGGCAACAATCTCCAC-3'.

Statistical Analysis

Data were expressed as mean \pm SD. Two group comparisons used 2-tailed Student's *t* tests. Multiple group data were evaluated with one-way ANOVA. *p* <0.05 was considered significantly different.

SUPPLEMENTAL INFORMATION

Supplemental Information can be found online at <https://doi.org/10.1016/j.omtn.2020.09.028>.

AUTHOR CONTRIBUTIONS

D.Z. conceived and designed the experiments. J.P., B.L., and X.L. carried out the experiments. H.L., J.L., analyzed the data. S.Q., X.X., and Z.D. contributed reagents/materials/analysis tools. D.Z. wrote the main manuscript text, but all authors reviewed the manuscript.

CONFLICTS OF INTEREST

The authors declare no competing interests.

ACKNOWLEDGMENTS

The study was supported, in part, by a grant from the National Natural Science Foundation of China (81870475, 81570646, and 81770951), Excellent Youth Foundation of Hu'nan Scientific Committee (2017JJ1035), and Changsha Science and Technology Bureau (kq1901115, kq2001039, kq1907144, and kq1901115).

REFERENCES

- Lafrance, J.P., and Miller, D.R. (2010). Acute kidney injury associates with increased long-term mortality. *J. Am. Soc. Nephrol.* *21*, 345–352.
- Matejovic, M., Valesova, L., Benes, J., Sykora, R., Hrstka, R., and Chvojka, J. (2017). Molecular differences in susceptibility of the kidney to sepsis-induced kidney injury. *BMC Nephrol.* *18*, 183.
- Murugan, R., Karajala-Subramanyam, V., Lee, M., Yende, S., Kong, L., Carter, M., Angus, D.C., and Kellum, J.A.; Genetic and Inflammatory Markers of Sepsis (GenIMS) Investigators (2010). Acute kidney injury in non-severe pneumonia is associated with an increased immune response and lower survival. *Kidney Int.* *77*, 527–535.
- Kiss, E., Czirják, L., and Szabó, G. (1988). [Retroperitoneal fibrosis in relation to three reported cases]. *Orv. Hetil.* *129*, 1857–1860.
- Izquierdo-García, J.L., Nin, N., Cardinal-Fernandez, P., Rojas, Y., de Paula, M., Granados, R., Martínez-Caro, L., Ruiz-Cabello, J., and Lorente, J.A. (2019). Identification of novel metabolomic biomarkers in an experimental model of septic acute kidney injury. *Am. J. Physiol. Renal Physiol.* *316*, F54–F62.
- Wei, S., Gao, Y., Dai, X., Fu, W., Cai, S., Fang, H., Zeng, Z., and Chen, Z. (2019). SIRT1-mediated HMGB1 deacetylation suppresses sepsis-associated acute kidney injury. *Am. J. Physiol. Renal Physiol.* *316*, F20–F31.
- Bellomo, R., Kellum, J.A., Ronco, C., Wald, R., Martensson, J., Maiden, M., Bagshaw, S.M., Glassford, N.J., Lankadeva, Y., Vaara, S.T., and Schneider, A. (2017). Acute kidney injury in sepsis. *Intensive Care Med.* *43*, 816–828.
- Mehta, T.K., Hoque, M.O., Ugarte, R., Rahman, M.H., Kraus, E., Montgomery, R., Melancon, K., Sidransky, D., and Rabb, H. (2006). Quantitative detection of promoter hypermethylation as a biomarker of acute kidney injury during transplantation. *Transplant. Proc.* *38*, 3420–3426.
- Guo, C., Pei, L., Xiao, X., Wei, Q., Chen, J.K., Ding, H.F., Huang, S., Fan, G., Shi, H., and Dong, Z. (2017). DNA methylation protects against cisplatin-induced kidney injury by regulating specific genes, including interferon regulatory factor 8. *Kidney Int.* *92*, 1194–1205.
- Wang, J., Li, H., Qiu, S., Dong, Z., Xiang, X., and Zhang, D. (2017). MBD2 upregulates miR-301a-5p to induce kidney cell apoptosis during vancomycin-induced AKI. *Cell Death Dis.* *8*, e3120.
- He, J., Zhang, B., and Gan, H. (2018). CIDEc Is Involved in LPS-Induced Inflammation and Apoptosis in Renal Tubular Epithelial Cells. *Inflammation* *41*, 1912–1921.

12. Duranton, C., Rubera, I., L'hoste, S., Cougnon, M., Poujeol, P., Barhanin, J., and Tauc, M. (2010). KCNQ1 K⁺ channels are involved in lipopolysaccharide-induced apoptosis of distal kidney cells. *Cell. Physiol. Biochem.* 25, 367–378.
13. Cunningham, P.N., Wang, Y., Guo, R., He, G., and Quigg, R.J. (2004). Role of Toll-like receptor 4 in endotoxin-induced acute renal failure. *J. Immunol.* 172, 2629–2635.
14. Guo, R., Wang, Y., Minto, A.W., Quigg, R.J., and Cunningham, P.N. (2004). Acute renal failure in endotoxemia is dependent on caspase activation. *J. Am. Soc. Nephrol.* 15, 3093–3102.
15. Wu, X., Guo, R., Chen, P., Wang, Q., and Cunningham, P.N. (2009). TNF induces caspase-dependent inflammation in renal endothelial cells through a Rho- and myosin light chain kinase-dependent mechanism. *Am. J. Physiol. Renal Physiol.* 297, F316–F326.
16. Khajevand-Khazaei, M.R., Mohseni-Moghaddam, P., Hosseini, M., Gholami, L., Baluchnejadmojarad, T., and Roghani, M. (2018). Rutin, a quercetin glycoside, alleviates acute endotoxemic kidney injury in C57BL/6 mice via suppression of inflammation and up-regulation of antioxidants and SIRT1. *Eur. J. Pharmacol.* 833, 307–313.
17. Raveh-Amit, H., Hai, N., Rotem-Dai, N., Shahaf, G., Gopas, J., and Livneh, E. (2011). Protein kinase C η activates NF- κ B in response to camptothecin-induced DNA damage. *Biochem. Biophys. Res. Commun.* 412, 313–317.
18. Xu, X., Wang, J., Yang, R., Dong, Z., and Zhang, D. (2017). Genetic or pharmacologic inhibition of EGFR ameliorates sepsis-induced AKI. *Oncotarget* 8, 91577–91592.
19. Havasi, A., and Borkan, S.C. (2011). Apoptosis and acute kidney injury. *Kidney Int.* 80, 29–40.
20. Chen, C.C., Wang, J.K., Chen, W.C., and Lin, S.B. (1998). Protein kinase C ϵ mediates lipopolysaccharide-induced nitric-oxide synthase expression in primary astrocytes. *J. Biol. Chem.* 273, 19424–19430.
21. Zurgil, U., Ben-Ari, A., Rotem-Dai, N., Karp, G., Krasnitsky, E., Frost, S.A., and Livneh, E. (2014). PKC η is an anti-apoptotic kinase that predicts poor prognosis in breast and lung cancer. *Biochem. Soc. Trans.* 42, 1519–1523.
22. Rotem-Dai, N., Oberkovitz, G., Abu-Ghanem, S., and Livneh, E. (2009). PKC ϵ confers protection against apoptosis by inhibiting the pro-apoptotic JNK activity in MCF-7 cells. *Exp. Cell Res.* 315, 2616–2623.
23. Li, X., Xu, L., Hou, X., Geng, J., Tian, J., Liu, X., and Bai, X. (2019). Advanced Oxidation Protein Products Aggravate Tubulointerstitial Fibrosis Through Protein Kinase C-Dependent Mitochondrial Injury in Early Diabetic Nephropathy. *Antioxid. Redox Signal.* 30, 1162–1185.
24. Chen, C., Liang, W., Jia, J., van Goor, H., Singhal, P.C., and Ding, G. (2009). Aldosterone induces apoptosis in rat podocytes: role of PI3-K/Akt and p38MAPK signaling pathways. *Nephron, Exp. Nephrol.* 113, e26–e34.
25. Gonçalves, G.L., Costa-Pessoa, J.M., Thieme, K., Lins, B.B., and Oliveira-Souza, M. (2018). Intracellular albumin overload elicits endoplasmic reticulum stress and PKC-delta/p38 MAPK pathway activation to induce podocyte apoptosis. *Sci. Rep.* 8, 18012.
26. Guo, Y., Song, Z., Zhou, M., Yang, Y., Zhao, Y., Liu, B., and Zhang, X. (2017). Infiltrating macrophages in diabetic nephropathy promote podocytes apoptosis via TNF- α -ROS-p38MAPK pathway. *Oncotarget* 8, 53276–53287.
27. Ge, Y., Wang, J., Wu, D., Zhou, Y., Qiu, S., Chen, J., Zhu, X., Xiang, X., Li, H., and Zhang, D. (2019). lncRNA NR_038323 Suppresses Renal Fibrosis in Diabetic Nephropathy by Targeting the miR-324-3p/DUSP1 Axis. *Mol. Ther. Nucleic Acids* 17, 741–753.
28. Xu, L., Li, X., Zhang, F., Wu, L., Dong, Z., and Zhang, D. (2019). EGFR drives the progression of AKI to CKD through HIPK2 overexpression. *Theranostics* 9, 2712–2726.
29. Sun, L., Zhang, D., Liu, F., Xiang, X., Ling, G., Xiao, L., Liu, Y., Zhu, X., Zhan, M., Yang, Y., et al. (2011). Low-dose paclitaxel ameliorates fibrosis in the remnant kidney model by down-regulating miR-192. *J. Pathol.* 225, 364–377.
30. Yang, R., Xu, X., Li, H., Chen, J., Xiang, X., Dong, Z., and Zhang, D. (2017). p53 induces miR199a-3p to suppress SOCS7 for STAT3 activation and renal fibrosis in UUO. *Sci. Rep.* 7, 43409.
31. Zhang, D., Pan, J., Xiang, X., Liu, Y., Dong, G., Livingston, M.J., Chen, J.K., Yin, X.M., and Dong, Z. (2017). Protein Kinase C δ Suppresses Autophagy to Induce Kidney Cell Apoptosis in Cisplatin Nephrotoxicity. *J. Am. Soc. Nephrol.* 28, 1131–1144.
32. Hedrich, C.M., Crispin, J.C., Rauen, T., Ioannidis, C., Apostolidis, S.A., Lo, M.S., Kyttaris, V.C., and Tsokos, G.C. (2012). cAMP response element modulator α controls IL2 and IL17A expression during CD4 lineage commitment and subset distribution in lupus. *Proc. Natl. Acad. Sci. USA* 109, 16606–16611.
33. Xu, X., Pan, J., Li, H., Li, X., Fang, F., Wu, D., Zhou, Y., Zheng, P., Xiong, L., and Zhang, D. (2019). Atg7 mediates renal tubular cell apoptosis in vancomycin nephrotoxicity through activation of PKC- δ . *FASEB J.* 33, 4513–4524.
34. Wang, J., Pan, J., Li, H., Long, J., Fang, F., Chen, J., Zhu, X., Xiang, X., and Zhang, D. (2018). lncRNA ZEB1-AS1 Was Suppressed by p53 for Renal Fibrosis in Diabetic Nephropathy. *Mol. Ther. Nucleic Acids* 12, 741–750.
35. Chen, J., Wang, J., Li, H., Wang, S., Xiang, X., and Zhang, D. (2016). p53 activates miR-192-5p to mediate vancomycin induced AKI. *Sci. Rep.* 6, 38868.
36. Zhang, T.N., Goodwin, J.E., Liu, B., Li, D., Wen, R., Yang, N., Xia, J., Zhou, H., Zhang, T., Song, W.L., and Liu, C.F. (2019). Characterization of Long Noncoding RNA and mRNA Profiles in Sepsis-Induced Myocardial Depression. *Mol. Ther. Nucleic Acids* 17, 852–866.